

COPY RIGHT



ELSEVIER
SSRN

2019IJIEMR. Personal use of this material is permitted. Permission from IJIEMR must be obtained for all other uses, in any current or future media, including reprinting/republishing this material for advertising or promotional purposes, creating new collective works, for resale or redistribution to servers or lists, or reuse of any copyrighted component of this work in other works. No Reprint should be done to this paper, all copy right is authenticated to Paper Authors

IJIEMR Transactions, online available on 4th Sept 2019. Link

[:http://www.ijiemr.org/downloads.php?vol=Volume-08&issue=ISSUE-09](http://www.ijiemr.org/downloads.php?vol=Volume-08&issue=ISSUE-09)

Title **A 3-Ø BALANCED DC-LINK MULTILEVEL INVERTER BY ABRIDGED AMOUNT OF DC SOURCES**

Volume 08, Issue 09, Pages: 459–471.

Paper Authors

N SANDEEP, P NAVEEN, P KALYAN

Anu Bose Institute of Technology K.S.P Road, New paloncha, Bhadradi Kothagudem, Telangana, India



USE THIS BARCODE TO ACCESS YOUR ONLINE PAPER

To Secure Your Paper As Per **UGC Guidelines** We Are Providing A Electronic Bar Code

A 3-Ø BALANCED DC-LINK MULTILEVEL INVERTER BY ABRIDGED AMOUNT OF DC SOURCES

N SANDEEP¹, P NAVEEN², P KALYAN³

^{1,2,3}UG Students, Dept. of Electrical and Electronics Engineering Anu Bose Institute of Technology
KSPRoad, Newpaloncha, Bhadradi Kothagudem, Telangana, India.
chanti7235@gmail.com¹, naveenpittala021@gmail.com², kalyanpilli00@gmail.com³

Abstract: - This paper displays a novel three-sort out DC-interface shocked inverter topology with diminished number of information DC power supplies. The proposed inverter incorporates strategy related half-partner modules to make the astonished waveform and a fundamental H-interface module, going about as a farthest point generator. The inverter yield voltage is moved to the store through a three-sort out transformer, which supports a galvanic withdrawal between the inverter and the heap. The proposed topology highlights different central focuses when separated and the standard flabbergasted inverters proposed in the academic works. These highlights combine adaptability, major control, decreased number of DC voltage sources and less contraptions check. A central sinusoidal heartbeat width balance philosophy is utilized to control the proposed inverter. The presentation of the inverter is overviewed under various stacking conditions and an appraisal with some present topologies is besides appeared. The presence of mind and adequacy of the proposed inverter are stated through reenactment and fundamental examinations utilizing a downsized low-voltage ask about office model.

Indexd Terms:-Hybridmultilevel inverter; DC-linkinverter; half-bridgemodule; symmetricDC voltage supply.

I.INTRODUCTION

Amazed inverters have gotten extraordinary thought from both insightful world and industry in the past couple of decades due to their specific features appeared differently in relation to their customary two-level accomplices [1, 2]. These fuse, lower trading mishaps and weight on the semiconductor contraptions, splendid yield waveforms, lessened electromagnetic impedance and more diminutive filtering necessities [3-6]. Fell Multilevel Inverters (CMLI) have gotten unprecedented tendency in various mechanical applications, especially, reasonable power source coordination [5, 7, 8]. This is especially due to their deliberate quality and reiteration incorporates close by the nonattendance of confounded capacitor

voltage modifying issue, which isa normal issue with various topologies, for instance, diodeandcapacitor caught inverters [9-11]. A couple of assortments of CMLI circuit topology havebeen accounted for in the open composition, wanting to fabricate the accomplished voltagelevels, which in the long run improvethe idea of the yield waveform [12]. Cross breed or hilter kilter fell stunned inverter is oneofthe proposed assortments, where distinctive information voltage levelsare ordinarily considered [13-16]. Diminished device check canbe cultivated with cream CMLIs, in any case nonappearance of estimated quality and conflicting voltage dispersal on thepower switchesmakes them revolting for utility-grade applications. Of course, another

genuine test with CMLIs is the prerequisite for nothing restricted DC power supplies, which power additional constraints and multifaceted nature, especially required. A couple of undertakings have been represented in the open composition intended to reduce the required number of the DC power supplies [11, 17-19]. For instance, [19-21] proposed another CMLI including scaffold cells arrange the unipolar staircase-shape waveform and a full-interface inverter as a furthest point generator. This has broadly diminished the contraptions count and the required number of DC power supplies differentiated and customary amazed inverters. Some changing capacitors are utilized inside the half-interface modules to reduce the amount of rectifiers in [19]. Anyway, as referenced in [11], changing these capacitors requires a jumbled control contrive. A growth of the topology proposed in [20, 21] was starting late point by point in [11], where a further diminishing in the required DC power supplies was practiced, in any case a possible development to three-arrange system was not uncovered. A segregated three-organize half-associate based CMLI is proposed in [22-24]. Regardless, these topologies require a higher number of isolated DC-supplies, which extends the cost and multifaceted nature similarly as the essential for a snared equalization methodology. Blend three-arrange CMLI is represented in [17, 18], where the fell half-interface cells are related with a three-organize voltage source inverter. This has basically diminished the amount of the semiconductor devices similarly as the required DC supplies. Nevertheless, the prerequisite for restricted DC power supplies couldn't be kept up a vital good ways from. Another assortment of the topologies considered in [11] was proposed

in [25, 26], where only a singular DC power supply is used and various degrees of the yield waveform were recognized through floating capacitors. Regardless, clearly this topology is significantly load-ward and requires propelled capacitor voltage modifying figurings, are tumbled to outline the stunned yield voltages, where the amount of levels is a component of the transformers' turns extents. Despite the way this has diminished the required DC power supplies, the huge number of single-arrange transformers makes it unfeasible and not charming as the size and multifaceted nature increases with every additional level in the yield voltage [11]. It pushes toward getting to be at any rate on different occasions when extended to three-arrange variation [17-20, 22]. As needs be, this paper proposes another symmetric three-arrange CMLI reliant on half-associate cells with decreased number of DC power supplies. This topology can be considered as an enlargement and update type of the three-arrange topology proposed in [19, 20]. Regardless, practically 30% more voltage levels in the line voltages can be cultivated by utilizing a comparative number of semiconductor devices. Section II displays the action rule of the proposed symmetric CMLI close by its guideline strategy. Zone III shows and looks at picked amusement and probably affirmed results. Assessment between the proposed topology and conventional CMLI is pulled in Section IV. Finally, the work is done up in Section V.

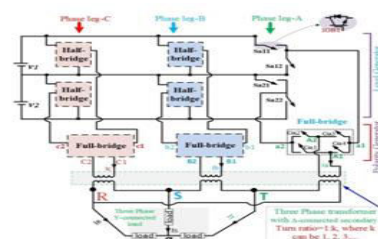


Fig. 1 the proposed three-phase CMLI with two half-bridge cells per phase leg

II. THE PROPOSED MULTILEVEL INVERTER AND ITS MODULATION STRATEGY

Figure 1 shows the proposed CMLI, incorporates 2 phases. The central stage is a level generator, which makes the unipolar stunted voltage waveforms by using the full half-ladder vital modules. As appeared in Fig. 1, every three half-interface modules in the three-sort out legs-A, B and C are proceeded from a non-kept DC power supply. Extremely, the DC-control supplies can be battery sources, or rectifier yield terminals. Besides, the DC supplies can be equivalently picked up from photovoltaic (PV) yield terminals or other supportable power source. To perceive suffering yield power and voltage for efficient power wellsprings of irregular qualities, some control figurings, for example, unsurprising voltage source mode can be utilized [29]. It is critical that the half-interface modules will have a practically identical blocking voltage fundamental since they are connected over a near DC-supply. This guarantees mien and fundamental control strategies. The ensuing stage is the uttermost point generator, which uses a reasonable full-partner inverter to bipolarize the paralyzed yield voltage waveforms passed on by the standard stage. A three-mastermind transformer couples the yields of the farthest point generator with the store, giving a galvanic partition correspondingly as boosting to the yield voltage. It ought to be seen that in spite of the path that in Fig. 1 the transformer right hand windings are related in Δ , it could be moreover related in Y, at whatever point required. In addition, the CMLI showed in Fig. 1 can be adequately reached out to make higher number of levels in the yield voltage waveform by including even more half-associate modules into the level generator.

$$m=2n+1 \quad (1)$$

$$v_1 = v_2 \dots = v_n = V_{DC} \quad (2)$$

Where VDC addresses a predictable worth While the half-interface modules in the level generator utilize low voltage, high trading repeat contraptions, the low repeat switches used in the full-associate modules in the furthest point generator experience a voltage stress of a size counterparts to the summation of the information DC voltage sources [20]. In this way, the voltage stress or standing voltage, V_{pg} , weight on the extremity generator switches can be communicated as,

$$V_{pg, stress} = nV_{DC} \quad (3)$$

It is to be seen that since they are working at the focal trading repeat of 50 Hz, full-associate modules don't demonstrate tremendous trading hardships. On the contrary side, top tier development right presently offers trading contraptions, for instance, Insulated Gate Bipolar Transistors (IGBT)- module, FZ500R65KE3 that can withstand a specialist to maker voltage up to 6.5 kV [30]. Additionally, the working voltage cutoff of the trading contraptions can be extended by partner various switches in course of action. Different CMLIs topologies utilizing half-augmentation and H-associate modules have been completed for high voltage applications and can be found in the artistic works [19, 31]. It justifies referencing that as the three-phase transformer is a fundamental part in the proposed topology, it will naturally fulfill the galvanic separation essential for reasonable power source grid related Applications

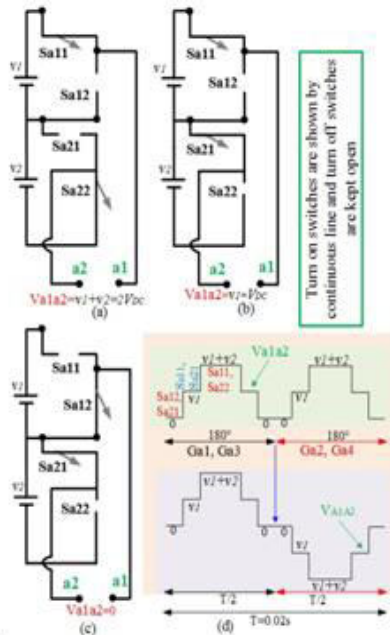


Fig. 2 switching logics for generating different levels in the level generator output voltages: (a) logic for generating $2V_{DC}$, (b) logic for generating V_{DC} , (c) logic for generating 0, (d) desired output in the level generator and polarity generator output voltage

Figures 2(a)- (c) demonstrate diverse exchanging conditions of the level generator, creating distinctive yield voltage levels (v_1+v_2 , v_1 , 0). Figure 2(d) represents the produced AC yield voltage in the extremity generator at stage leg-A, where the extremity generator flips the waveform every 180°. The primary focal point of this article is to build up another inverter topology. Customary Sinusoidal Pulse-Width Modulation (SPWM) system is a notable and simple to actualize strategy [32]. Henceforth, SPWM is embraced to show the viability of the proposed topology. As appeared in Fig. 3, the reference signals, Ref-a, Ref-b, Ref-c are the corrected sinusoidal waveforms with a 120° stage move from one another. These are then contrasted and two transporter signals (bearer 1 and transporter 2) to produce the required gating signals. Same exchanging signals age rationale is used for each stage leg.

III. SEMICONDUCTOR LOSSES AND CONVERTER EFFICIENCY

The semiconductor misfortunes are considered as a vital structure and determination measure for any converter circuit as they impact and characterize the required warm administration, which adds the estimation of the general cost/volume/weight of the inverter. There are two predominant misfortunes in the semiconductor gadgets; the static and the dynamic misfortunes. The on-state obstruction and the forward voltage drop of these semiconductor gadgets are in charge of the conduction misfortunes, while the dynamic misfortunes are delivered during the turn on/off activities managed by the exchanging recurrence of the device.

$$\begin{aligned} \sigma_{c,T}(t) &= [V_T + R_T i^\beta(t)]i(t) \\ \sigma_{c,D}(t) &= [V_D + R_D i(t)]i(t) \end{aligned} \quad (4)$$

Where, the on-state voltage drops of the transistor and diode are communicated by V_T and V_D , separately. The on-state protections of the transistor and diode, are given by R_T and R_D , correspondingly. β and $i(t)$ are the transistor enhancement factor and a transistor or diode current at any moment of time, separately.

Henceforth, the normal conduction misfortunes in both, the transistor and the diode, meant by $P_{c,T}(t)$ and $P_{c,D}(t)$, respectively are given by:

$$\begin{aligned} P_{c,T}(t) &= \frac{1}{2\pi} \int_0^{2\pi} [(V_T + R_T i^\beta(t))i(t)] d(\omega t) \\ P_{c,D}(t) &= \frac{1}{2\pi} \int_0^{2\pi} [(V_D + R_D i(t))i(t)] d(\omega t) \end{aligned} \quad (5)$$

The total average conduction losses can then be calculated from,

$$P_c(t) = \int_0^{2\pi} [(N_{Transistor}(t) * P_{c,T}(t)) + \{N_{Diode}(t) * P_{c,D}(t)\}] d(\omega t) \quad (6)$$

where $N_{Transistor}$ and N_{Diode} are the number of transistors and diodes, respectively, in the same current path at any instant of time.

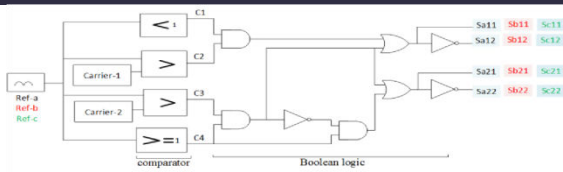


Fig. 3 Block diagram of the modulation technique

$$\left. \begin{aligned}
 E_{on} &= \int_0^{t_{on}} v(t)i(t)dt \\
 &= \int_0^{t_{on}} \left[\left(\frac{V_{sw}}{t_{on}} * t \right) \left(-\frac{I}{t_{on}} \right) * (t - t_{on}) \right] dt \\
 &= \frac{1}{6} V_{sw} * I * t_{on} \\
 E_{off} &= \int_0^{t_{off}} v(t)i(t)dt \\
 &= \int_0^{t_{off}} \left[\left(\frac{V_{sw}}{t_{off}} * t \right) \left(-\frac{I'}{t_{off}} \right) * (t - t_{off}) \right] dt \\
 &= \frac{1}{6} V_{sw} * I' * t_{off}
 \end{aligned} \right\} (7)$$

where V_{sw} and I , represent the off-state voltage and current of the device, respectively. I' represents the device current measured just before the device is turned off. The total switching power losses (P_{sw}), for a time-period T can be calculated from,

$$P_{sw} = \frac{1}{T} [\sum_1^{N_{switch}} \{ (N_{on} * E_{on}) + (N_{off} * E_{off}) \}] \quad (8)$$

where the number of turn-on and off counts of a switch in a cycle is given by N_{on} and N_{off} ; respectively.

The overall semiconductor losses of the proposed CMLI can be estimated by the total conduction and switching losses of all used semiconductors, expressed as:

$$P_{total_loss} = P_{con} + P_{sw} \quad (9)$$

If the output power is P_{out} , the inverter efficiency (η) can be calculated from:

$$\eta\% = \left(\frac{P_{out}}{P_{total_loss} + P_{out}} \right) * 100\% \quad (10)$$

Where the output power is calculated from:

$$P_{out} = \sqrt{3} * \frac{3V_{dc}}{\sqrt{2}} * \frac{I_{line}}{\sqrt{2}} * PF \quad (11)$$

TABLE I: PROPERTIES SYSTEM SPECIFICATIONS OF THE PROPOSED INVERTER

Input DC sources (v_1, v_2)	60V each
Carrier frequency	4 kHz
Switching controller	TMS320F2812
Ratings of IGBT	HGTG20N60B3D
Magnitudes of the line voltages	270V (peak)
Number of levels in line voltages	13

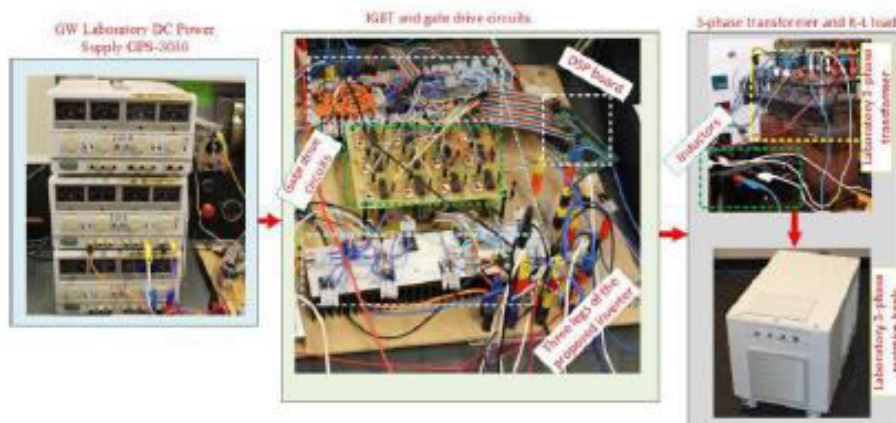


Fig. 4 Experimental test-rig setup

IV. SIMULATION AND EXPERIMENTAL RESULTS

Fig. 4 shows the trial test-apparatus of the proposed inverter, created at the Green Electric Energy Park (GEEP), Curtin University [33]. Then again, reproduction examination is completed utilizing the

Matlab/Simulink programming bundle. The principle parameters of the inverter model are condensed in Table 1. The information DC voltages from the 'GW Laboratory DC power supplies GPS-3030' are set to give a steady DC voltage of 60V, for example ($v_1=v_2=60$ volts). Both, the level generator

and extremity generator stages require twelve IGBTs, each. An advanced sign processor (DSP), TMS320F2812 is utilized to create the constant exchanging door signals. The door signals from the DSP are associated with the IGBT entryways through 24-entryway drive circuits. The job of entryway drive circuits is to detach the shared conviction of the DSP yield door heartbeats and lift up their sizes to almost 15 volts. As appeared in Fig. 4, there are two printed circuit sheets including 24-entryway drive circuits for the 24 IGBTs in the level generator and extremity generator stages. In this paper, the customary SPWM balance technique is considered with a transporter recurrence of 4kHz for both, reproduction and test thinks about. The adjustment record M_i is communicated as [32].

$$M_i = \frac{A_m}{(N_p - 1)A_c} \quad (12)$$

where A_m is the greatness of the reference sine waveform and A_c is the size of the bearer signal. Regulation file, M_i has an effect on the extent of the yield line voltages and line flows [32]. The yield of the extremity generator is associated with the essential of a three-stage segregation transformer with a turn proportion of 1:1, as appeared in Fig. 4.

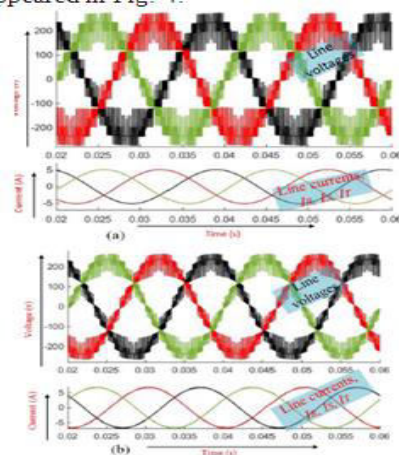


Fig. 5 Simulation results of the output line voltages and line currents for (a) load of nearly 0.8-lagging power factor and (b) load of nearly unity power factor

$$\begin{bmatrix} V_{RS} \\ V_{ST} \\ V_{TS} \end{bmatrix} = \frac{1}{3} \begin{bmatrix} 2 & -1 & -1 \\ -1 & 2 & -1 \\ -1 & -1 & 2 \end{bmatrix} \begin{bmatrix} V_{C1C2} \\ V_{B1B2} \\ V_{A1A2} \end{bmatrix} \quad (13)$$

$$\begin{bmatrix} V_{RS} \\ V_{ST} \\ V_{TS} \end{bmatrix} = \begin{bmatrix} 1 & -1 & 0 \\ 0 & 1 & -1 \\ -1 & 0 & 1 \end{bmatrix} \begin{bmatrix} V_{C1C2} \\ V_{B1B2} \\ V_{A1A2} \end{bmatrix} \quad (14)$$

The performance of the proposed inverter under various loading conditions is assessed as elaborated in the following case studies.

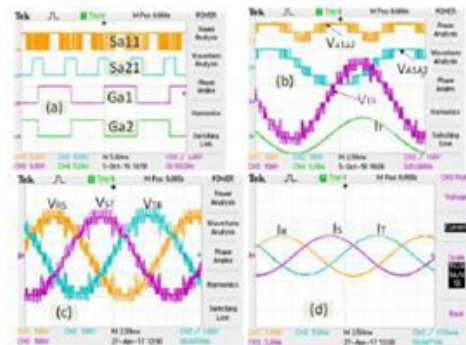


Fig. 6 Different experimental results for phase leg-A with a load of nearly 0.8 lagging power factor: (a) gate pulses in half-bridge and full bridge module at phase leg-A, (b) level and polarity generator output voltages along with the line voltage and line current for phase leg-A, (c) three phase line voltages and (d) three phase line currents.

A. Case study 1: The impact of load power factor

Fig. 5 shows the simulated results of the line voltage and line current waveforms of the proposed inverter under load power factor of nearly 0.8 (lagging) and unity power factor, when each phase leg is connected with balanced inductive loads of $(20+j15.7\Omega)$ and $(20+j1.57\Omega)$, respectively.

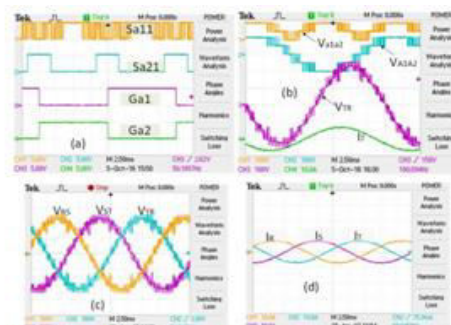


Fig. 7 Different experimental results for phase leg-A with a load of nearly unity power factor: (a) gate pulses in half-bridge and full bridge module at phase leg-A, (b) level and polarity generator output voltages along with the line voltage and line current for phase leg -A, (c) three phase line voltages and (d) three phase line currents.

Then again, Figs.6&7 outline distinctive trial results for about 0.8 slacking and solidarity power factor loads, individually. Tektronix TPS2014B advanced capacity oscilloscope is used for catching the exploratory waveforms and showing their symphonious ranges. It merits referencing that, no consonant channels were used while taking the outcomes. Figs.6(a)&7(a) represent the test gating signals for both, the level generator and extremity generator switches, Sa11, Sa21, Ga1, Ga2 in stage leg-A. The comparing level generator yield voltage (Va1a2) the extremity generator yield voltage (VA1A2), line voltage (VTR) and line current (IT) are appeared in Figs.6(b)&7(b). Also, Figs. 6(c), 6(d) and 7(c), 7(d) demonstrate the 3 stage line voltages and line flows, individually.

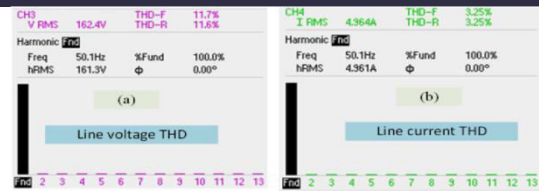


Fig. 9 THD results for nearly unity PF load:
(a) THD for line voltage waveform,
(b) THD for line current waveform

It merits referencing that the inductance of an inductive burden goes about as a line current symphonious channel [34], thus, the line current contains sounds on account of 0.8 slacking PF load instead of solidarity PF load. The THD of the line current waveforms is under 5% in both stacking conditions, which fulfills the IEEE standard [35]. Then again, the estimation of voltage THD is not exactly the fell MLI proposed in [18-20, 22]. The line voltage THD can be kept inside worthy point of confinement, if a little channel is associated at the yield terminals or through expanding the quantity of levels in the line voltages by falling all the more half-connect cells in each stage leg.

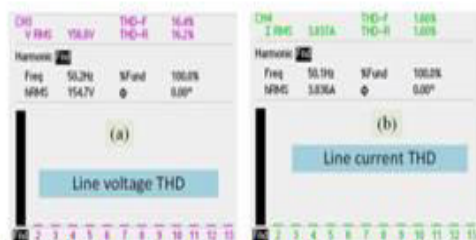


Fig. 8 THD results for nearly 0.8 lagging PF load:
(a) THD for line voltage waveform,
(b) THD for line current waveform

The all out symphonious twists (THD) of the line voltage and line current waveforms of the two cases above are appeared in Figs. 8 and 9, separately. It tends to be seen that the difference in the heap PF from 0.8 slacking to solidarity does not impact the quantity of levels in the line voltage waveforms. Be that as it may, the THD in the line voltage and line current waveforms is changed because of the adjustment in the heap PF.

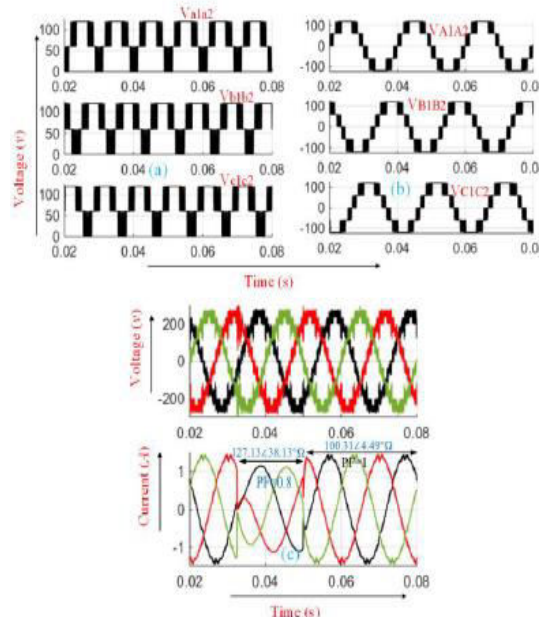


Fig. 10 Simulation results for a dynamic change in the load from nearly unity PF (100.31∠4.49°Ω) to 0.8 lagging PF (127.13∠38.13°Ω): (a) level generator output voltage, (b) polarity generator output voltage (phase voltage) and (c) line voltage and line current

B. Casestudy 2: Theperformance of inverter underload dynamics

Inverter yield voltage¤t waveforms are seen during burden dynamic conditions. Fig.10 demonstrates the reproduction results when a heap of almost solidarity powerfactor ($100+j7.85\omega$ per stage leg) changed at $t=0.0325s$ to $100+j78.5\omega$ per stage leg. It is expected that this change goes on for a span of $0.0175s$ after which the first burden is held.

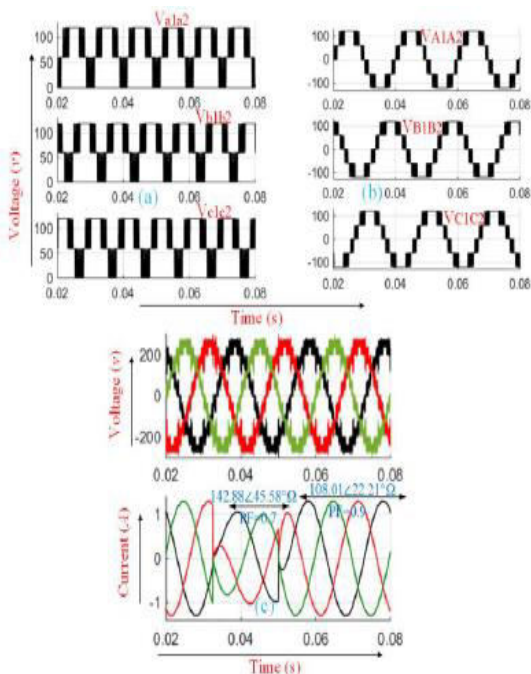


Fig. 11 Simulation results for a dynamic change in the load from nearly 0.9 lagging PF ($108.01\angle 22.21^\circ\Omega$) to 0.7 lagging PF ($142.88\angle 45.58^\circ\Omega$): (a) level generator output voltage, (b) polarity generator output voltage (phase voltage) and (c) line voltage and line current

In spite of the fact that a little mutilation can be seen in the line voltage waveforms in Fig. 10(c) during the change time frame, no impact is found on the level generator yield voltages appeared in Figs. 10(a)&10(b). Comparable perception can be found in Fig. 11 when a heap of $100+j40.82\omega$ per stage leg changes to $100+j102.05\omega$ per stage leg at $t=0.0325s$ for a term of $0.0175s$.

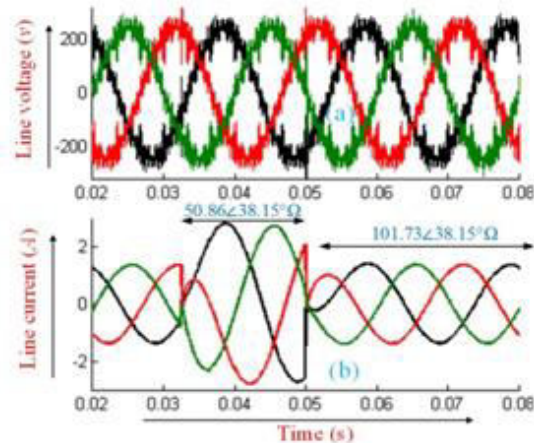


Fig. 12 Simulation results for a dynamic change in the load magnitude with the same PF: (a) Line voltage, (b) Line current

The presentation of the proposed CMLI is likewise examined with an adjustment in the heap size with a similar power factor. Fig. 12 demonstrates the inverter line voltage and line current waveforms when the heap is multiplied at $t=0.0325s$ for a term of $0.0175s$. Same perceptions in the over two cases can be seen for this situation study also.

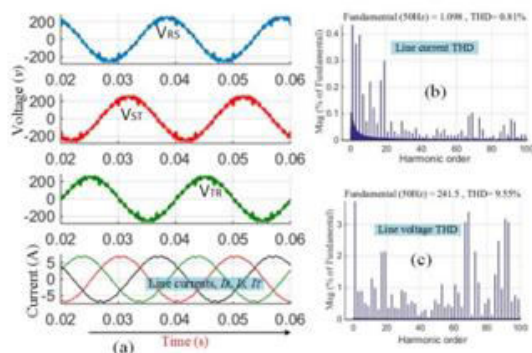


Fig. 13 Simulation results for carrier frequency of 8 kHz: (a) line voltages and currents, (b) line current THD, (c) line voltage THD

C. Case study 3: Impact of changing the carrier frequency on the inverter performance

To evaluate the exhibition of the proposed inverter with high bearer recurrence, the transporter recurrence is expanded from 4 kHz to 8 kHz. Fig. 13 demonstrates the inverter's yield line voltages and line flows at 8 kHz bearer recurrence and a heap of

20+j15.7ω Fig. 11 Simulation results for a powerful change in the heap from about 0.9/stage leg. For this situation, the THD of the line voltage and line slacking PF (108.01 22.21°ω) to 0.7 slacking PF (142.88 45.58°ω): (a) level generator yield voltage, (b) extremity generator yield voltage (stage)

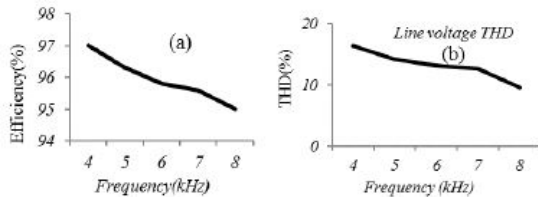


Fig. 14 Effect of carrier frequency on (a) Semiconductor efficiency, (b) Line voltage THD

The efficiency of the proposed inverter and the quality of the line voltage waveforms are evaluated in a wide range of carrier frequencies. Figs. 14(a) & 14(b) show the THD of the line voltage waveforms and inverter semiconductor efficiency for a set of carrier frequencies. While the quality of the line voltage waveforms is found better for higher carrier frequencies, semiconductor efficiency degrades with higher frequencies due to increased switching losses.

Table 2: Inverter Performance At Different Modulation Index (Based On Simulation Results)

Modulation index	0.6	0.7	0.8	0.9	1
Inverter efficiency (%)	76	80	94	95	97
Peak line voltage (V)	190	200	210	250	270
Peak line current (A)	3.3	3.54	3.8	4.6	5.2
THD _{line voltage} (%)	38.11	36.92	34	23.3	15.6
THD _{line current} (%)	3.62	2.51	2.14	1.53	1.37

A wide scope of SPWM exchanging recurrence (1 kHz to 12 kHz) has been. A wide scope of the proposed in the writing for various staggered inverter topologies [19, 22, 36, 37]. The ideal exchanging recurrence is an exchange of between exchanging misfortunes and the nature of the yield voltage and henceforth the size of the framework. As indicated by Fig. 14(a), to keep up the proficiency of the proposed

current waveforms is decreased from 15.6% and 1.37% if there should be an occurrence of (c) line voltage and line current 4 kHz bearer recurrence to 9.55% and 0.81%; individually if there should be an occurrence of 8 kHz transporter recurrence.

inverter at 97% or over, a bearer recurrence of 4 kHz is considered. The productivity will be diminished to 95.8% if a transporter recurrence of 6 kHz is utilized. Then again, the line voltage THD comparing to 4 kHz bearer recurrence is 15.6% while it marginally decreased to 13.14% with a transporter recurrence of 6 kHz. Thus, for the proposed topology a transporter recurrence of 4 kHz gives an attractive execution as far as inverter effectiveness and nature of the yield waveforms. At this recurrence, the THD in the line current was observed to be 1.37% according to the above contextual investigations.

D. Case study 4: Impact of Modulation index

Tab 2 demonstrates the inverter proficiency and the extents of the inverter yield line voltage and line current for various balance files, M_i when the inverter is stacked by 20+j15.7ω in each stage leg and worked at a transporter recurrence of 4 kHz. Effectiveness essentially diminished when M_i is under 0.8. Table 2 likewise demonstrates that while the sizes of the line voltage and line current increment with the expansion of the regulation record, the THD in the two waveforms is diminishing.

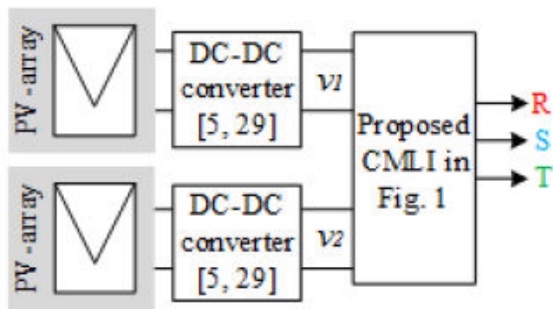


Fig. 15 Simplified block diagram for PVCMLI -application of the proposed

E. Casestudy 5: photovoltaic application

As referenced of segment II, the information DC supplies can be acquired from photovoltaic yield terminals or other sustainable power source. For situation study the achievability of the proposed inverter with PV framework is surveyed. The exhibition of the proposed inverter is researched supplanting the two info

DC power supplies in Fig. 1 by two PV modules. A square graph of PV-cluster associated with the proposed CMLI in this paper is appeared in Fig. 15. DC-DC converter is used to keep up the DC voltages v_1 and v_2 at consistent levels according to the control approach proposed in [5, 29]. It is accepted that a steady voltage control calculation as introduced in [5, 29] used to keep up the PV-modules yield voltage at 80 volts as appeared in Fig. 16(a). With a heap of $20 + j15.7\omega$, the MLI yield line voltage waveforms are as appeared in Fig. 16(b). The quantity of levels and the THD of the yield line voltage waveforms stay unaltered contrast with yield waveforms delineated in Casestudy 1.

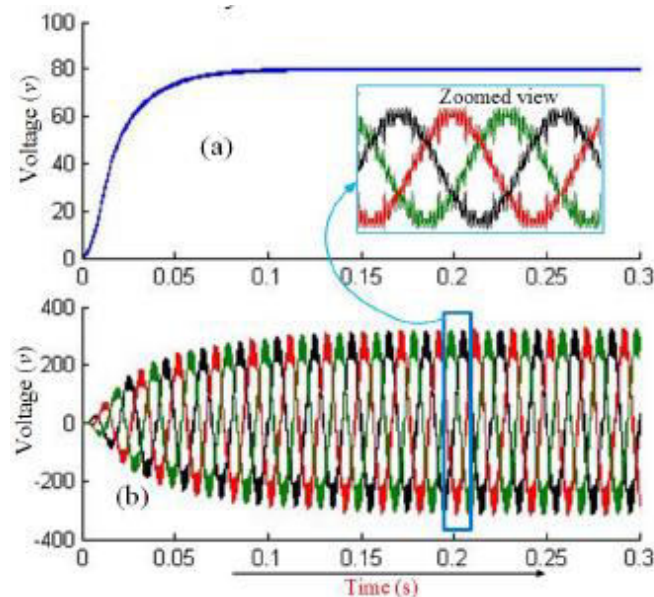


Fig. 16 PV application: (a) PV module output voltage, (b) proposed inverter output line voltage

Notwithstanding their application in PV control transformation, half-bridge module based staggered inverters have been additionally used for medium voltage and electric vehicle applications as announced in [18, 38]. It is normal that the topology proposed in this paper likewise be used for the

previously mentioned applications and give extra points of interest, for example galvanic disengagement and decreased info DC-voltage supplies. As indicated by makers' information sheets [39] used three-stage transformer is of high effectiveness (up to 99%).

TABLE 3
COMPARISON BETWEEN THE PROPOSED TOPOLOGY AND CONVENTIONAL MLI

	Diode clamped	Flying Capacitor	CHB	Proposed CMLI
Number of clamping diodes [20]	$3*(m-1)*(m-2)$	0	0	0
Number of clamping capacitors [20]	0	$3(m-1)*(m-2)/2$	0	0
Number of voltage divider capacitors [20]	$3*(m-1)$	$3*(m-1)$	0	0
Number of switching devices [20]	$6*(m-1)$	$6*(m-1)$	$6*(m-1)$	$3*(m+3)$
Number of DC supplies [20]	1	1	$3(m-1)/2$	$(m-1)/2$
Output Transformer [28]	1	1	1	1
Inverter Efficiency [40] [41] [42]	Up to 96%	Up to 97%	Up to 95%	97%

Consequently, the general proficiency of the proposed inverter won't fundamentally influence an examination with other existing half-bridge based CMLI. Also, as this topology requires less number of intensity electronic gadgets in contrast with other full topologies, the general misfortunes are relied upon to be diminished.

V. COMPARISON WITH OTHER MLI TOPOLOGIES

A. Comparison with conventional topologies

Table 3 demonstrates a general correlation between the proposed CMLI and traditional MLI for example diode clamped, flying capacitor and full H-connection topologies regarding the gadget count (an element of the quantity of levels in the yield voltage, m) and by and large productivity. In opposite with ordinary MLI, Table 3 demonstrates that the proposed CMLI does

is the principle issue of customary diode clamped and flying capacitor topologies [20]. The table additionally demonstrates that the proposed topology requires $3(m+3)$ exchanging gadgets, while other topologies require $6(m-1)$ exchanging gadgets. Subsequently, for any number of levels over 5, the proposed CMLI will require a minimal number of exchanging gadgets. Besides, the proposed CMLI requires less number of DC supplies than the CHB inverter.

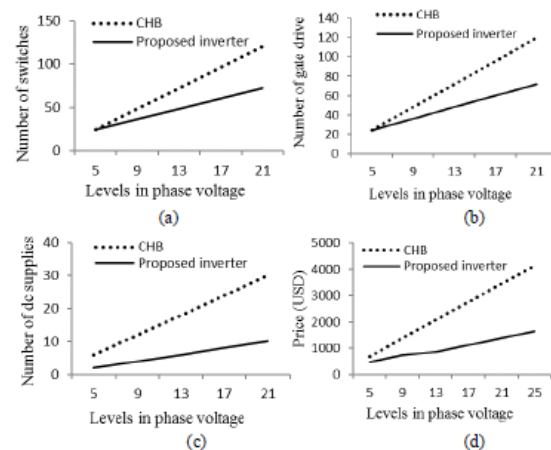


Fig. 17 Device counts and cost comparison with CHB: (a) number of switching devices, (b) number of gate drivers, (c) number of DC power supplies, (d) cost comparison per phase voltage level

In Fig. 17, it demonstrates a correlation between the proposed inverter & ordinary three-phase H-connection (CHB) inverter [42, 43] as a function of the quantity of levels m in the yield voltage waveform. As shown in Fig. 17(a-c), the execution of the proposed inverter calls for a lesser number of intensity electronic switches, door drive circuits, and DC supplies. Fig. 17(d) demonstrates a cost comparison between the proposed CMLI and traditional CHB-based MLI to get 1.5 kV (top) in the line voltage. Cost estimation incorporates IGBT modules, entryway drivers, and full-connection rectifiers and depends on 2017 market costs [44]. It merits referencing that a three-stage transformer is a fundamental part in the regular staggered inverters for high-power lattice reconciliation to give the required galvanic confinement [28]. Consequently, the detachment

transformer in the proposed topology in this article does not acquire additional cost when the proposed full inverter is used as a framework associated PV inverter. Fig. 17 demonstrates that the proposed topology is a financially savvy decision when contrasted and the regular CHB staggered inverter topologies.

B. Comparison with other half-bridge based topologies

The fundamental accentuation of the proposed inverter planned for amplifying the quantity of yield voltage levels with diminished number of DC voltage supplies by using the symmetry properties. In this manner, it is basic to contrast the proposed topology and other proportionate half-bridge based topologies announced in the writings [18,19,22] affirm its prevalence. As condensed from Table 4, unique angles are considered to draw a reasonable correlation, this incorporates: the quantity of half-bridge cells, complete number of intensity electronic exchanging gadgets, door drive circuits, number of DC-control supplies or DC-interface capacitors, number of the feasible yield voltage levels in the line voltages. As can be found in Table 4, the proposed topology accomplishes higher number of yield voltage levels by using a similar number of intensity electronic exchanging gadgets and door drive circuits. Strangely, the proposed full staggered inverter in this paper requires the least number of DC supplies than some other topology introduced in Table 4.

VI. CONCLUSION

This paper demonstrates another symmetrical advanced inverter topology with 2 particular stages. The proposed inverter requires less power electronic contraptions and features estimated quality, in this way direct structure, less cost, & high versatility. The amount of data DC-supplies for the

when contrasted and topologies proposed in [18, 19, 22].

In particular, the topology proposed in [22], requires more than double the quantity of absolute exchanging gadgets, entryway drive circuits and DC supplies for producing lower number of levels in the line voltage contrasted and the proposed topology in this paper. Then again, in spite of the fact that the topology proposed in [18], requires less number of symmetric half-bridge cells, it just produces seven-levels in the yield line voltage. The topology proposed in [18] would require 7 symmetric half-bridge modules in each stage leg to create 13-level at the yield line voltage, which is accomplished in the proposed topology in this paper by just utilizing 3 symmetric half-bridge modules. This implies, 42-exchanging gadget alongside 19 DC-control supplies will be required, if the topology proposed in [18], is reached out to produce 13-levels in the line voltage.

TABLE 4 COMPARISON OF THE PROPOSED THREE-PHASE SYMMETRIC HALF-BRIDGE TOPOLOGY WITH OTHER HALF-BRIDGE TOPOLOGIES PROPOSED IN THE LITERATURES

	Proposed topology in this paper	Three phase topology proposed in [19]	Three phase topology proposed in [22]	Three phase topology proposed in [18]
No of half-bridge cells	6	6	15	9
No of total switching devices	24	24	42	18
No of gate driver	24	24	42	18
No of DC supplies or capacitors	2	6	15	9
No levels in the line voltage	13	9	11	7

proposed topology is seen to be practically 67% not actually the tantamount symmetric half-bridge topologies, which is a remarkable achievement for present day applications. This miracle diminishes multifaceted design of DC voltage the administrators. Like a symmetric structure, all the trading devices experience same voltage stress, which is a critical factor for high voltage applications. The believability of the proposed inverter is insisted through reenactment and

exploratory assessment for different working conditions.

REFERENCES

1. L.G.Franquelo, J.Rodriguez, J.I.Leon, S.Kouro, R. Portillo, and M. A. Prats, "The period of staggered converters arrives," *IEEE India Electronmagazine*, volume 2, pp. 28-39, 2008.
2. Nabae, I. Takahashi, H. Akagi, "Another nonpartisan pointclamped PWM inverter," *IEEE Trans. Ind. Appl.*, pp. 518-523, 1981.
3. S.Kouro, M.Malinowski, K.Gopakumar, J.Pou, L.G.Franquelo, B.Wu, et al., "Ongoing advances and mechanical uses of staggered converters," *IEEE Trans. Ind. Electron.*, vol. 57, pp. 2553-2580, 2010.
4. B.Xiao, L.Hang, J.Mei, C.Riley, L.M.Tolbert, and B. Ozpineci, "Measured full H-bridge staggered PV inverter with circulating MPPT for matrix associated applications," *IEEE Trans. Ind. Appl.* vol. 51, pp. 1722-1731, 2015.
5. J.Pereda, J.Dixon, "High-recurrence interface: an answer for utilizing just a single dc source in lopsided full staggered inverters," *IEEE Trans. Ind. Electron.*, vol. 58, pp. 3884-3892, 2011.
6. M.R. Islam, G. Youguang, and Z. Jianguo, "A high-recurrence interface staggered full medium-voltage converter for direct lattice joining of sustainable power source frameworks," *IEEE Trans. Power Electron.*, vol. 29, pp. 4167-4182, 2014.
7. H. Akagi, "Arrangement, wording, and utilization of the modular staggered current converter (MMCC)," *IEEE Trans. Power Electron.*, vol. 26, pp. 3119-3130, 2011.
8. N. Kawakami, S. Ota, H. Kon, S. Konno, H. Akagi, H. Kobayashi, et al., "Improvement of a 500-kW particular staggered current converter for battery vitality stockpiling frameworks," *IEEE Trans. Ind. Appl.*, vol. 50, pp. 3902-3910, 2014.